

# The developing heat transfer and fluid flow in micro-channel heat sink with viscous heating effect

Dorin Lelea · Adrian Eugen Cioabla

Received: 8 June 2010 / Accepted: 9 December 2010 / Published online: 30 January 2011  
© Springer-Verlag 2011

**Abstract** The numerical modeling of the conjugate heat transfer and fluid flow through the micro-heat sink was presented in the paper, considering the viscous dissipation effect. Three different fluids with temperature dependent fluid viscosity are considered: water, dielectric fluid HFE-7600 and isopropanol. The square shape of the cross-section is considered with  $D_h = 50 \mu\text{m}$  with a channel length  $L = 50 \text{ mm}$ . As most of the reported researches dealt with fully developed fluid flow and constant fluid properties in this paper the thermal and hydro-dynamic developing laminar fluid flow is analyzed. Two different heat transfer conditions are considered: heating and cooling at various Br. The influence of the viscous heating on local Nu and Po is analyzed. It was shown that for a given geometry the local Po and Nu numbers are strongly affected by the viscous heating. Moreover the Po number attains the fully developed value as the external heating is equal with the internal viscous heating.

## List of symbols

Br	Brinkman number
$c_p$ , J/kg K	Specific heat
$D_h$ , m	Hydraulic diameter
$f$	Darcy friction factor
$k$ , W/mK	Thermal conductivity
$L$ , m	Length
Nu	Nusselt number
Po	Poiseuille constant

$Q$ , W	Heat transfer rate
$q$ , W/m <sup>2</sup>	Heat flux
$Re$	Reynolds number
$T$ , K	Temperature
$u$ , $v$ , m/s	Velocity components
$M$ , kg/s	Mass flow rate
$x$ , $z$	Spatial coordinates

## Greek symbols

$\Phi$	Viscous dissipation term
$\mu$	Pa s, Viscosity
$\rho$ , kg/m <sup>3</sup>	Density

## Subscripts

ave	Average
i	Inner
in	Inlet
out	Outlet
o	Outer
s	Solid
f	Fluid
w	Wall

## 1 Introduction

The miniaturization of devices in electronics industry, biomedical applications or process industry raised the interest in microchannel heat transfer and fluid flow. The fundamentals of the microchannel heat transfer and fluid flow are essential for a proper design of these devices. On the other hand, as the scale of the system is decreasing below a certain value, some effects like temperature dependent properties or viscous dissipation has a considerable influence on thermal and hydrodynamic behavior.

D. Lelea (✉) · A. E. Cioabla  
Department of Thermal Machines and Transportation,  
Faculty of Mechanical Engineering,  
University Politehnica Timisoara, B-dul Mihai Viteazu nr. 1,  
300222 Timisoara, Romania  
e-mail: ldorin@mec.upt.ro

Arici et al. [1] made a numerical study related with thermally developing the laminar forced convection in a pipe including the wall conductance and viscous dissipation. The viscous dissipation is found to affect both the wall and bulk fluid temperature profiles. Significant viscous dissipation effects have been observed for large Br. Its effect becomes more pronounced downstream.

Koo et al. [2] studied the effects of viscous dissipation on the temperature field and also on the friction factor using dimensional analysis and experimentally validated computer simulations for three different working fluids (water, methanol and iso-propanol) in micro-tubes and micro-channels. The variation of temperature with the Reynolds number was studied for rectangular channels and there was made a comparison between the experimental data and the computational results.

Celata et al. [3] analyzed the issue of scaling effects that cause influential effects when channel geometry is reduced below a certain limit. The results were connected with the role of viscous heating in micro-channel flows, its occurrence in the Navier Stokes equations and also there was made an experimental validation for verifying its presence in practice. The experimental results were compared with the values existing in literature for compliance.

Rands et al. [4] investigated experimentally the laminar-turbulent transition for water flow in circular microtubes with diameters in the range 16.6–32.2  $\mu\text{m}$  and  $Re = 300$ –3,400. The fluid temperature rise, due to viscous dissipation, increases with increasing microtube length and decreasing microtube diameter. The viscous heating-induced temperature rise is significant, reaching 35°C in some cases.

Nonino et al. [5] analyzed numerically the effects of viscous dissipation and temperature dependent viscosity in both thermally and simultaneously developing laminar flows of liquids in straight microchannels of arbitrary, but constant, cross-sections. It was shown that, both temperature dependence of viscosity and viscous dissipation effects cannot be neglected in a wide range of operative conditions. In all the computations, the same values of the Reynolds and Prandtl numbers,  $Re = 500$  and  $Pr = 5$  at the reference temperature of the fluid have been assumed.

Chen [6] performed forced convection flow in micro-channels with viscous dissipation effect and slip flow regime. It was found that when the viscous dissipation effect is considered the Nu is increasing and then reaches its final value. It also produces a noticeable increase in the fully developed Nusselt number.

Judy et al. [7] investigated pressure driven liquid flow through round and square microchannels fabricated from fused silica and stainless steel. Regarding the viscous heating effect, the maximum rise in liquid temperature was

6.2°C, found at the maximum Reynolds number tested  $Re = 300$ .

Hooman et al. [8, 10], analyzed theoretically the role of viscous dissipation on forced convection, with temperature-dependent viscosity and thermal conductivity, through microchannels and micropipes, under isoflux wall boundary condition. The analytical results can be used for macrochannels where continuum assumption, and hence, no-slip condition is still valid.

van Rij et al. [9] studied numerically the effect of viscous dissipation and rarefaction on rectangular micro-channel convective heat transfer rates, subject to  $H_2$  and  $T$  thermal boundary conditions. Both analytical and numerical data indicate that effects of viscous dissipation, flow work, and axial conduction are all significant within the slip flow regime for thermally/hydrodynamically developing and locally fully developed Nusselt numbers.

Morini [11] analyzed theoretically the limit of significance for viscous dissipation effects in microchannel flows. The role of the cross-sectional geometry on viscous dissipation as well as the minimum Reynolds number for which viscous dissipation effects can no longer be neglected for fluid flow in micro-channels were determined. It was found that viscous heating decreases the fluid viscosity, so the friction factor decreases as the Reynolds number increases.

Tunc and Bayazitoglu [12] investigated the convective heat transfer for steady laminar hydrodynamically developed flow in microtubes with temperature jump at the wall and viscous heating conditions. It was concluded that Nusselt number takes higher values for cooling and lower for heating.

Magyari and Barletta [13] analyzed analytically laminar forced convection flow of a liquid in the fully developed region of a pipe with viscous dissipation effect and temperature dependent viscosity.

Jeong [14] investigated the extended Graetz problem in a flat channel including effects of rarefaction, streamwise conduction and viscous dissipation. The flow is assumed to be fully developed with temperature developing profile. It was shown the Nusselt number decreases as Knudsen number or Brinkman number increases and as Peclet number decreases.

El-Genk and Yang [15] examined the experimental measurements in an attempt to quantify the effect of a potential slip on the reported values of Poiseuille number, determined from the pressure drop measurements in the experiments. It was concluded that the results of recent investigations suggest that a nonslip boundary may not be valid in highly confined and stressed flows.

Yeoun and Yogesh [16] presented the numerical report on conjugate heat transfer during the optical fiber coating

process in an axisymmetric applicator considering the viscous dissipation. It was found that the temperature level increased with the fiber speed due primarily to the tremendous viscous dissipation within the fluid at higher speeds, especially in the die.

Hung [17] performed the second law analysis to investigate the influence of viscous dissipation in fully developed forced convection for single-phase liquid flow in a circular microchannel under imposed uniform wall heat flux. It is found that, under certain conditions, the effect of viscous dissipation on entropy generation in microchannel is significant and should not be neglected.

The latest research reports revealed the fact that viscous dissipation cannot be neglected at the microscale. At some circumstances the effect of viscous heating could affect the classic behaviors of the convective parameters like Nu or Po numbers. Most of the research reports presented above consider the fully developed flow and only a few of them take into account the variable fluid viscosity and simultaneously developing heat transfer and fluid flow.

Considering these arguments, the present research report deals with numerical modeling of the thermal and hydrodynamic developing laminar fluid flow and heat transfer in the square microchannel-heat sink for  $Re < 2,100$  and  $Pr = 5-30$ . The variable fluid viscosity and viscous dissipation term in the energy equation, were considered. Three different fluids have been considered water, HFE-7600 and

isopropanol during cooling and heating to emphasize the behavior of the local Nu and Po numbers.

## 2 Numerical details

The one-layer microchannel heat sink is presented in the Fig. 1. Due to the symmetry plane, the half cross-section of one channel is considered in computations. The conventional set of the Navier-Stokes equations has been used for the conjugate laminar steady state heat transfer and fluid flow, as follows:

The continuity equation:

$$\frac{\partial u}{\partial x} + \frac{\partial v}{\partial y} + \frac{\partial w}{\partial z} = 0 \tag{1}$$

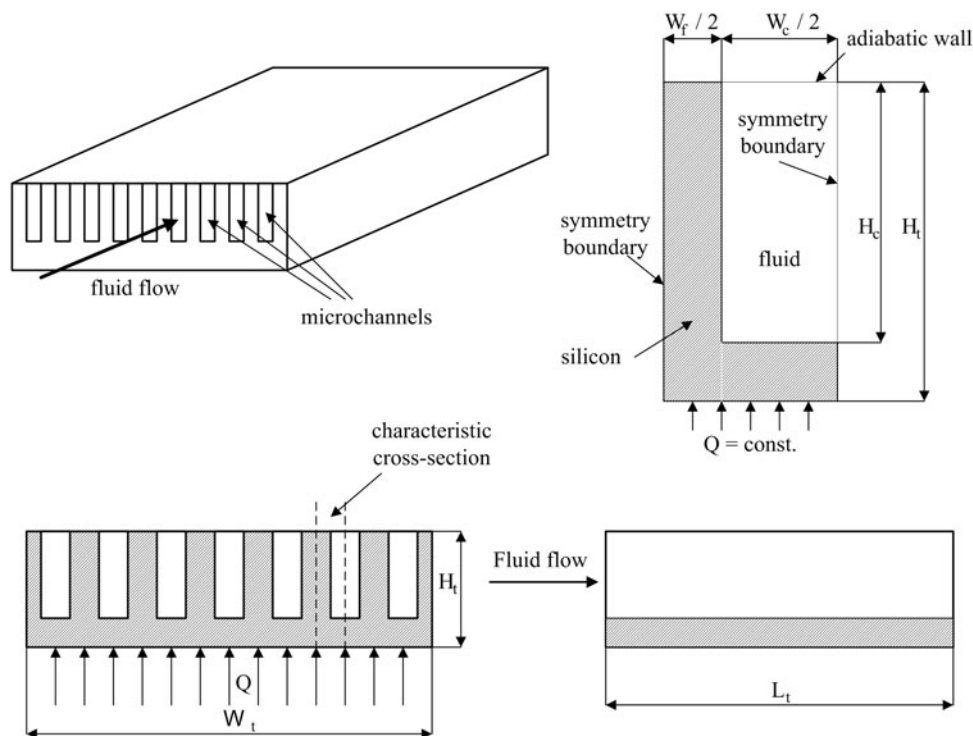
The momentum equation:

$$\rho \left( u \frac{\partial u}{\partial x} + v \frac{\partial u}{\partial y} + w \frac{\partial u}{\partial z} \right) = -\frac{dp}{dz} + \left( \frac{\partial}{\partial x} \left( \mu \frac{\partial u}{\partial x} \right) + \frac{\partial}{\partial y} \left( \mu \frac{\partial u}{\partial y} \right) \right) \tag{2}$$

$$\rho \left( u \frac{\partial v}{\partial x} + v \frac{\partial v}{\partial y} + w \frac{\partial v}{\partial z} \right) = -\frac{\partial p}{dx} + \left( \frac{\partial}{\partial x} \left( \mu \frac{\partial v}{\partial x} \right) + \frac{\partial}{\partial y} \left( \mu \frac{\partial v}{\partial y} \right) \right) \tag{3}$$

$$\begin{aligned} \rho \left( u \frac{\partial w}{\partial x} + v \frac{\partial w}{\partial y} + w \frac{\partial w}{\partial z} \right) \\ = -\frac{\partial p}{dy} + \left( \frac{\partial}{\partial x} \left( \mu \frac{\partial w}{\partial x} \right) + \frac{\partial}{\partial y} \left( \mu \frac{\partial w}{\partial y} \right) \right) \end{aligned} \tag{4}$$

**Fig. 1** The microchannel heat sink, calculation domain and cross-sections



The energy equation (for both fluid and solid):

$$\rho \cdot c_p \cdot \left( u \frac{\partial T}{\partial x} + v \frac{\partial T}{\partial y} + w \frac{\partial T}{\partial z} \right) = k \left( \frac{\partial^2 T}{\partial x^2} + \frac{\partial^2 T}{\partial y^2} + \frac{\partial^2 T}{\partial z^2} \right) + \Phi \quad (5)$$

where viscous dissipation term is defined as:

$$\Phi = \mu \cdot \left\{ 2 \cdot \left[ \left( \frac{\partial u}{\partial x} \right)^2 + \left( \frac{\partial v}{\partial y} \right)^2 + \left( \frac{\partial w}{\partial z} \right)^2 \right] + \left( \frac{\partial v}{\partial x} + \frac{\partial u}{\partial y} \right)^2 + \left( \frac{\partial w}{\partial y} + \frac{\partial v}{\partial z} \right)^2 + \left( \frac{\partial u}{\partial z} + \frac{\partial w}{\partial x} \right)^2 \right\} \quad (6)$$

The fluid properties are constant except for fluid viscosity that is evaluated with the following equations: for water:

$$\mu(t) = 2.6412018 \times 10^{-4} + 0.0014009 \cdot e^{-\frac{t}{31.0578605}} \quad (7)$$

for dielectric fluid HFE-7600 [18]:

$$\mu(t) = (1587.5 - 1.755 \cdot t) \times 10^{-6} \cdot e^{\frac{464.403382}{t+133} - 2.881482} \quad (8)$$

for isopropanol:

$$\mu(T) = 4.266 \cdot 10^{-7} T^2 - 3.016 \cdot 10^{-4} \cdot T + 5.398 \cdot 10^{-2} \quad (9)$$

The thermal conductivity of the silicon substrate is  $k_s = 148$  W/mK. The following boundary conditions are prescribed for the system of the partial differential equations:

The conjugate heat transfer procedure, implies the continuity of the temperature and heat flux at the solid–liquid interface defined as,

$$x = W_f/2 : T_s|_{x+} = T_f|_{x-}$$

$$k_s \left( \frac{\partial T_s}{\partial x} \right)_{x+} = k_f \left( \frac{\partial T_f}{\partial x} \right)_{x-}$$

$$y = H_t - H_c : T_s|_{y+} = T_f|_{y-}$$

$$k_s \left( \frac{\partial T_s}{\partial y} \right)_{y+} = k_f \left( \frac{\partial T_f}{\partial y} \right)_{y-}$$

For the heated portion of the microchannel the following boundary condition is defined:  $y = 0$ :

$$q_o = k_s \frac{\partial T}{\partial y}$$

Also at the inlet cross-section, uniform velocity and temperature field are considered:  $z = 0$ :

$$u = u_{in} \text{ and } T = T_{in}$$

The upper boundary is isolated defined as:

$$k_s \frac{\partial T}{\partial y} = 0$$

At the outlet of the microchannel the following boundary conditions are prescribed:

$$z = L_t$$

$$\frac{\partial T}{\partial z} = 0; \quad \frac{\partial u}{\partial z} = 0; \quad v = w = 0$$

At the symmetry boundary:

$$x = w_f/2 + w_c/2$$

$$v = 0; \quad \frac{\partial w}{\partial x} = 0; \quad \frac{\partial u}{\partial x} = 0; \quad \frac{\partial T}{\partial x} = 0$$

$$x = 0$$

$$\frac{\partial T}{\partial z} = 0$$

The microchannel heat sink dimensions are presented in the Table 1.

The solution procedure is based on the method used in [19] for microtubes and on the Finite Volume Method described in [20]. First, the parabolic flow field condition is considered and the velocity field is solved. The temperature field, as a conjugate heat transfer problem, was then solved as the elliptic problem using the obtained velocity field. Also  $k$  acts as  $k_s$  for silicon wall and  $k_f$  in the case of the fluid. At the fluid–solid interface  $k$  is calculated as the harmonic mean value. The velocity–pressure coupling is solved using a SIMPLER method. A staggered grid is used for cross-stream velocities with power-law discretization scheme. The results of the grid sensitivity testing for water and  $Re = 2,100$  are presented in Fig. 2. It is observed that a difference between a coarser ( $15 \times 30 \times 100$ ) and finer grid ( $25 \times 40 \times 180$ ) is below 0.1% for bulk temperature and less than 1% for average wall temperature. So, the first one is used for the rest of calculations.

Darcy friction factor is defined by the following equation:

$$f = \frac{-(dp/dz) \cdot D_h}{\rho \cdot u_m^2/2} \quad (10)$$

and a  $Re$  is defined as:

$$Re = \frac{\rho \cdot u_m \cdot D_h}{\mu} \quad (11)$$

So, from (5) and (6) the local Po can be obtained in the following form:

$$Po = f Re = \frac{-2 \cdot (dp/dz) \cdot D_h^2}{u_m \cdot \mu} \quad (12)$$

**Table 1** The geometric data and working parameters of the microchannel heat sink

$w_f$ $\mu\text{m}$	$w_c$ $\mu\text{m}$	$H_c$ $\mu\text{m}$	$H_t$ $\mu\text{m}$	$L_h$ cm	$L_t$ cm	$w_t$ cm	$q$ W/cm <sup>2</sup>	$Re$
36	50	50	100	5	5	1.5	35	200–2,100

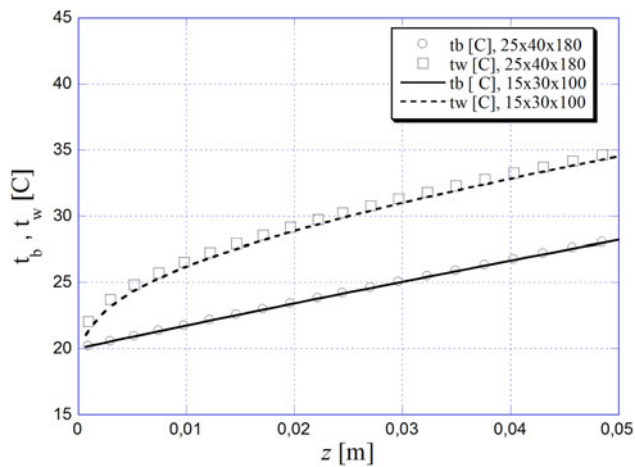


**Fig. 2** The temperature distribution along the micro-heat sink for two grids

While the local Nu number is defined with the following equation:

$$\text{Nu} = \frac{h_{\text{ave}} \cdot D_h}{k} \quad (13)$$

Where the average heat transfer coefficient, based on the peripherally averaged heat flux and wall temperature, is defined as:

$$h_{\text{ave}} = \frac{q|_{\Gamma}}{t_w|_{\Gamma} - t_b}$$

The conjugate heat transfer and fluid flow of the micro-channel heat sink was analyzed also by Li et al. [21] and Lee and Garimella [22] with averaged Nu.

The Brinkman number for constant wall heat flux is defined as:

$$\text{Br} = \frac{u_m^2 \cdot \mu}{q \cdot D_h} \quad (14)$$

The Br has the positive value for heating and negative for cooling. The viscosity in this case is evaluated at the inlet temperature.

### 3 Results and discussion

In the Fig. 3 the temperature variation along the micro-channel has been presented for isopropanol and conditions presented in [7] (square microchannel with  $D_h = 74.1 \mu\text{m}$ ,  $L = 11.4 \text{ cm}$  and  $Re = 300$ ). A difference between the outlet temperature obtained by the numerical code and the experimental outlet temperature is about 3%. The code validation was also made with experimental results for average Po with viscosity based on the inlet temperature (Fig. 4). The excellent agreement between the present numerical results and experimental results [7] is observed

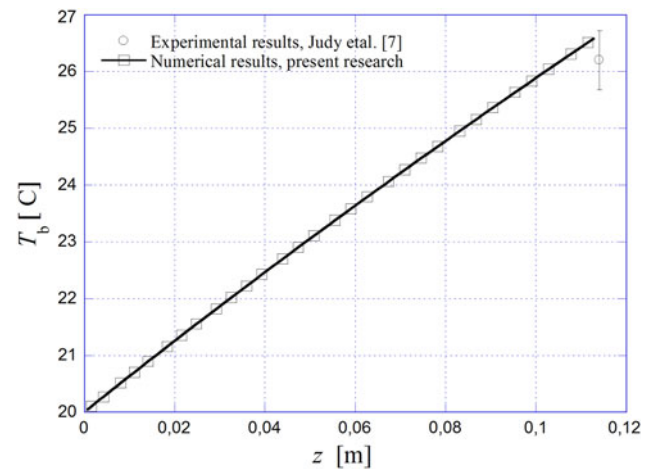


**Fig. 3** The bulk temperature distribution along the micro-heat sink for isopropanol

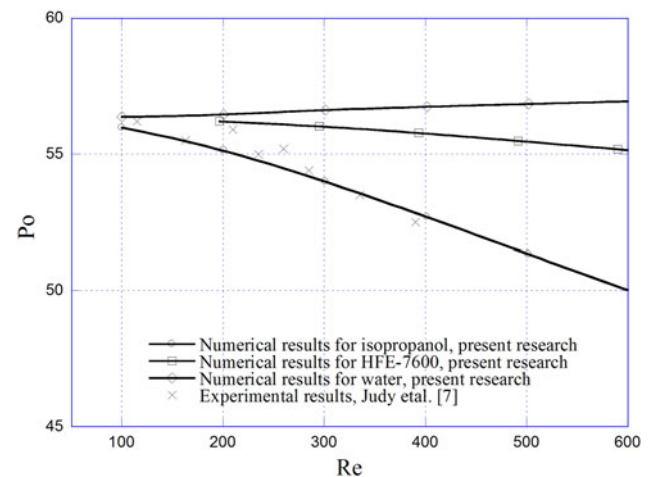


**Fig. 4** The Po variation versus  $Re$  for water, HFE-7600 and isopropanol, present numerical results compared with experimental results [7]

with a maximum difference of 3%. In the same figure the average Po variation with  $Re$  is presented for water and HFE-7600. For dielectric fluid HFE-7600 the Po is decreasing with  $Re$  but at the lower rate compared with isopropanol, because of the lower viscosity. Contrary to isopropanol and HFE-7600, the Po is slightly increasing with  $Re$  for water.

The local Po distribution is presenting in the Figs. 5, 6 and 7 for three working fluids. It is observed that Po is decreasing along the microchannel due to the temperature dependent viscosity. Moreover as the Br is increasing the local Po is increasing in case of heating.

On the other hand for the cooling case, the local Po is increasing for low  $\text{Br} = -0.002$ . As the Br is increasing the local Po is approaching the constant value in the fully developed region. It has to be stated that a fully developed

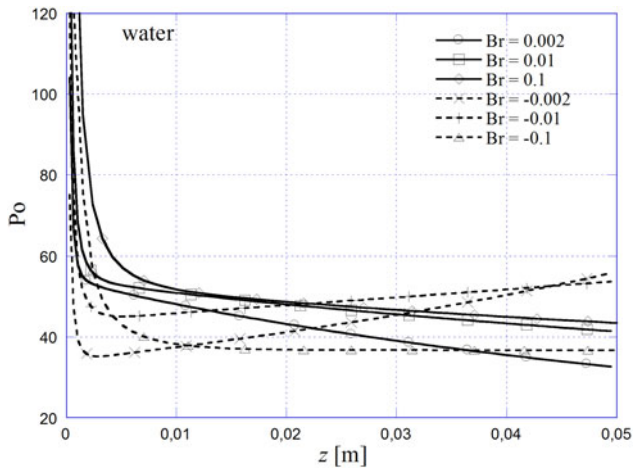


**Fig. 5** The local  $Po$  variation along the micro-heat sink for water, various  $Br$  and two heat flux directions (heating and cooling)

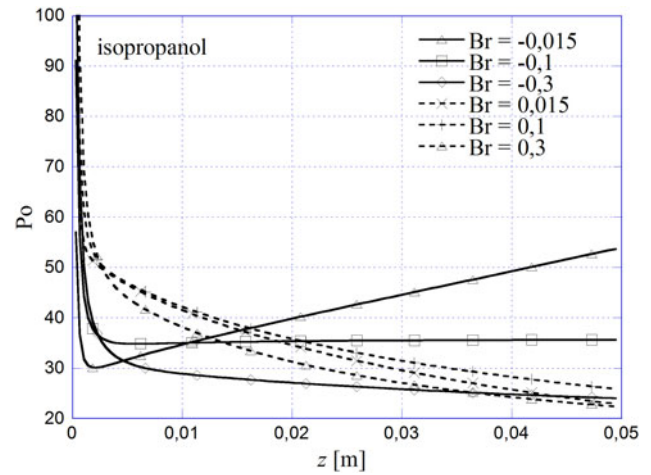


**Fig. 7** The local  $Po$  variation along the micro-heat sink for isopropanol, various  $Br$  and two heat flux directions (heating and cooling)

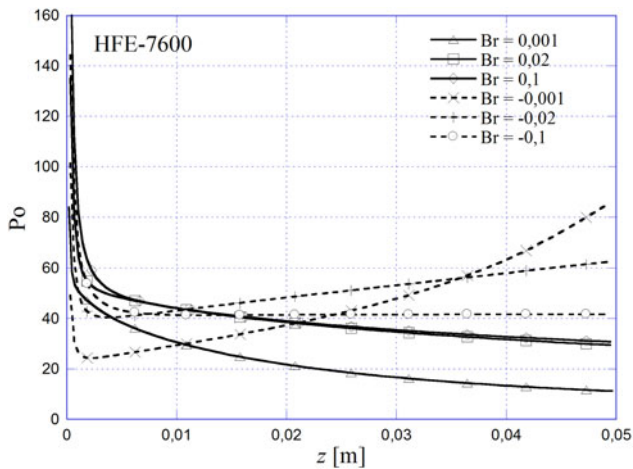


**Fig. 6** The local  $Po$  variation along the micro-heat sink for HFE-7600, various  $Br$  and two heat flux directions (heating and cooling)

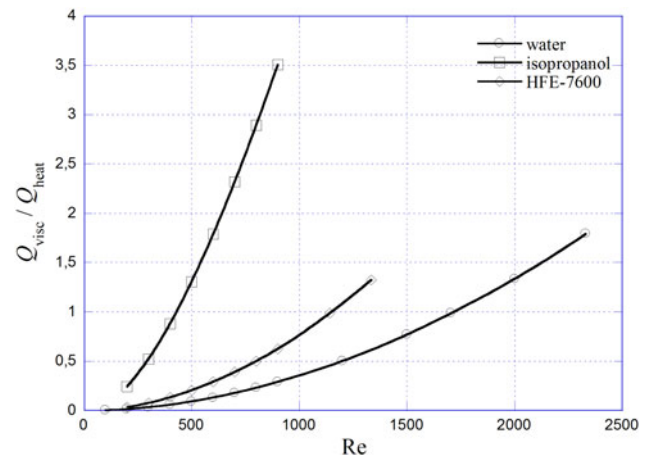


**Fig. 8** The merit of the viscous heating for water, isopropanol and HFE-7600

$Po$  is lower than the conventional value for the square channel ( $Po = 56.908$ ).

The plausible explanation for the fully developed  $Po$  at a fixed  $Br$  is related to the ratio between the heat transfer rate due to viscous dissipation and sensible heat dispersed through the bottom wall of the micro-heat sink. At a certain value of  $Br$  (or  $Re$ ) the ratio between the viscous heating and external cooling is equal to 1. In the Fig. 8 the ratio between the heat transfer rate from viscous heating and external heating (or cooling) versus  $Re$  is presented. The heat transfer rate ratio is equal to unity at  $Re = 430$  for isopropanol, at  $Re = 1,140$  for HFE and at  $Re = 1,800$  for water.

On the other hand, the fully developed values are observed for water at  $Re = 1,800$ , for HFE-7600 at  $Re = 1,330$  and for isopropanol at  $Re = 480$ . Obviously these values are in the range of the heat transfer rate equal to unity.

In the Figs. 9, 10 and 11 the peripherally averaged local  $Nu$  versus axial distance is presented. It is difficult to compare the fully developed values for local  $Nu$  in the case of the conjugate heat transfer due to the different heating of the side walls. This issue is more complicated in the presence of viscous heating due to the additional internal heat source. The peripherally average local  $Nu$  exhibits the boundary layer flow approaching the fully developed value. For water (Fig. 9) and low  $Br = 0.002$  ( $-0.002$ ) the local  $Nu$  is approaching the conventional fully developed  $Nu_{fd} \cong 3.608$ . As the  $Br$  is increasing to 0.01 ( $-0.01$ ) the fully developed value is still preserved with the longer thermal entrance effect. If the  $Br$  is increasing to 0.1 the thermal entrance length is increasing and the fully developed value is decreasing to  $Nu_{fd} \cong 2.67$ . In the case of cooling  $Br = -0.1$ , both the thermal entrance length and fully developed  $Nu_{fd} \cong 5.42$  are increasing. Deviation

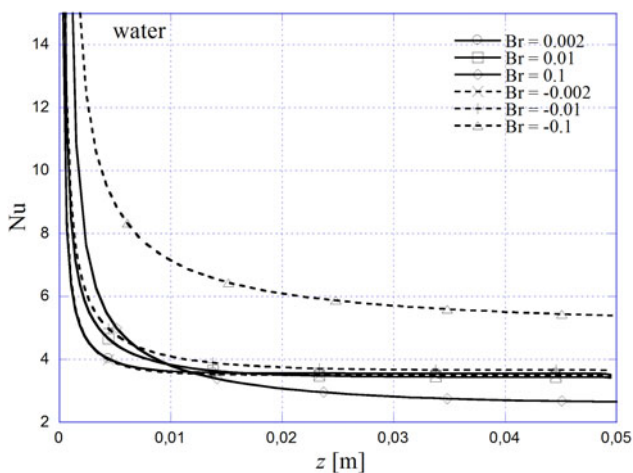


Fig. 9 The local Nu versus axial distance for water

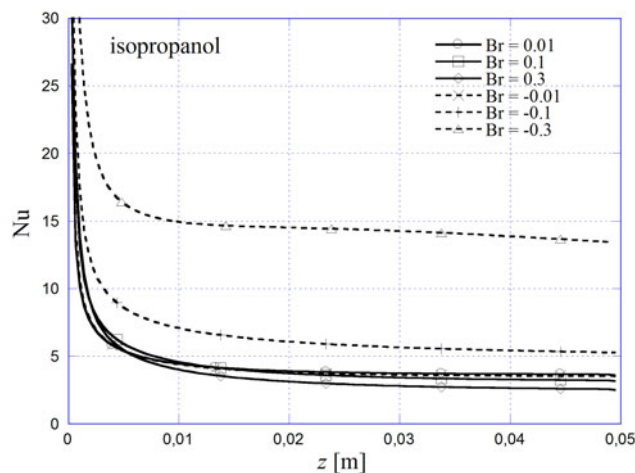


Fig. 11 The local Nu versus axial distance for isopropanol

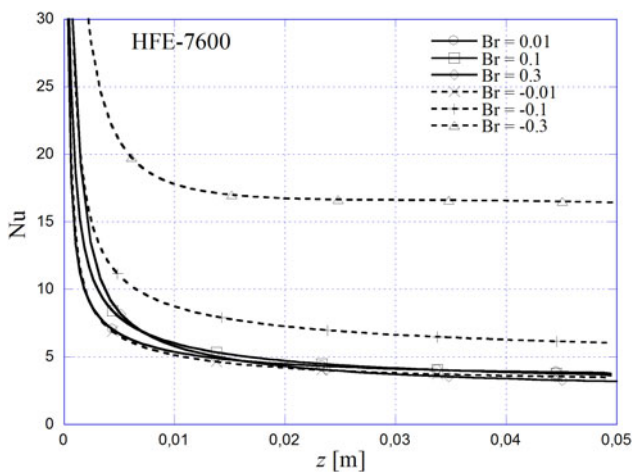


Fig. 10 The local Nu versus axial distance for HFE-7600

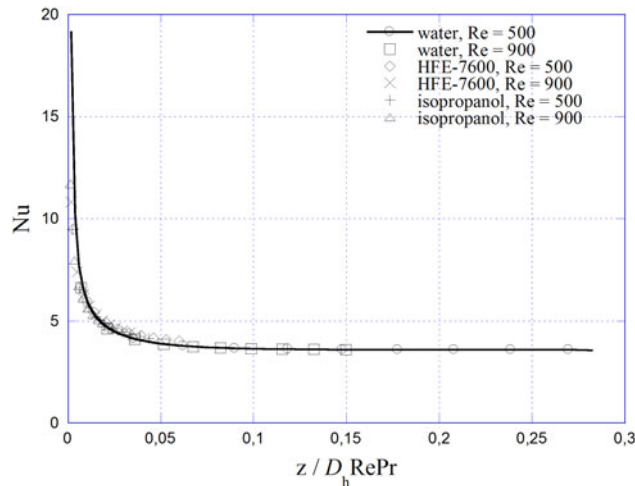


Fig. 12 The local Nu versus non-dimensional axial distance for water, HFE-7600 and isopropanol

from the conventional fully developed value is induced by the temperature difference between the wall and fluid, that increases for heating and decreases in the case of cooling. As the fluid is heating, the wall temperature increases more rapidly than a bulk fluid temperature due to the combined effect of temperature dependent viscosity and viscous heating. Consequently the temperature difference is increasing as the  $Re$  or  $Br$  is increasing and  $Nu$  number is decreasing. The reverse case is true for the cooling case.

In the Fig. 10 the local  $Nu$  distribution along the microchannel is presented for HFE-7600 and various  $Br$ . The similar behavior of the local  $Nu$  is observed for higher  $Br$ , except for cooling cases. For  $Br = -0.1$  the fully developed local  $Nu_{fd} \cong 6.15$  is obtained while for  $Br = -0.3$  the fully developed  $Nu_{fd} \cong 16.53$ . Once again the thermal entrance length is increasing.

The local  $Nu$  versus axial distance is presented for isopropanol in the Fig. 11. The conventional fully developed value  $Nu_{fd} \cong 3.608$  is observed for  $Br = 0.01$  ( $-0.01$ ). If the

$Br$  is increasing to 0.1 the fully developed  $Nu_{fd} \cong 3.17$  is decreasing, while for  $Br = 0.3$  further decreasing of the  $Nu_{fd} \cong 2.5$  is observed. In the case of cooling and  $Br = -0.1$ , the fully developed  $Nu_{fd} \cong 5.38$  is obtained while for  $Br = -0.3$  the fully developed  $Nu_{fd} \cong 13.46$  is increasing. In the latter case the local  $Nu$  is slightly decreasing with axial distance in the fully developed region.

In the Fig. 12 the local  $Nu$  versus non-dimensional axial distance for water, HFE-7600 and isopropanol versus  $Re$  is presented for non-viscous heating case. The conventional behavior of the local  $Nu$  is observed with the fully developed  $Nu_{fd} \cong 3.608$ .

### 4 Conclusions

The numerical modeling of the simultaneously developing heat and fluid flow in the microchannels with effects of

viscous dissipation was discussed. The special attention is focused on a local  $Nu$  and  $Po$  for three working fluids: water, HFE-7600 and isopropanol with temperature dependent viscosity covering the range  $Pr = 5–30$ . The following conclusions are outlined:

- The local  $Po$  decreases with  $Re$  for isopropanol and HFE-7600 and increases for water as the viscosity is evaluated at the inlet temperature of the fluid.
- The local  $Po$  relation is affected by the viscous dissipation for all Br. As the Br is increasing the local  $Po$  is increasing along the microchannel as the fluid is cooled and decreasing as the fluid is heating.
- For a certain value of Br the local  $Po$  is achieving the fully developed value as for the non-heating case. The plausible explanation is that the heat transfer rate of the internal source due to viscous heating is equal to the heat transfer rate due to external heat source.
- In the case of thermal results there is a different behavior of local  $Nu$  depending on the heat flux direction (heating or cooling). If the fluid is heating the local  $Nu$  is decreasing while for cooling the local  $Nu$  is increasing. A deviation from the conventional value  $Nu_{fd} \cong 3.608$  is higher as the fluid is cooled.

**Acknowledgments** This work was supported by CNCSIS –UEFI-SCSU, project number 670 PNII – IDEI 938/2008.

## References

1. Arici ME, Aydin O (2009) Conjugate heat transfer in thermally developing laminar flow with viscous dissipation effects. *Heat Mass Transf* 45:1199–1203
2. Koo J, Kleinstreuer C (2004) Viscous dissipation effects in microtubes and microchannels. *Int J Heat Mass Transf* 47:3159–3169
3. Celata GP, Morini GL, Marconi V, McPhail SJ, Zummo G (2006) Using viscous heating to determine the friction factor in microchannels—an experimental validation. *Exp Therm Fluid Sci* 30:725–731
4. Rands C, Webb BW, Maynes D (2006) Characterization of transition to turbulence in microchannels. *Int J Heat Mass Transf* 49:2924–2930
5. Nonino C, Giudice SD, Savino S (2007) Temperature-dependent viscosity and viscous dissipation effects in simultaneously developing flows in microchannels with convective boundary conditions. *J Heat Transfer* 129:1187–1194
6. Chen CH (2006) Slip-flow heat transfer in a microchannel with viscous dissipation. *Heat Mass Transf* 42:853–860
7. Judy J, Maynes D, Webb BW (2002) Characterization of frictional pressure drop for liquid flows through microchannels. *Int J Heat Mass Transf* 45:3477–3489
8. Hooman K, Ejlali A (2010) Effects of viscous heating, fluid property variation, velocity slip, and temperature jump on convection through parallel plate and circular microchannels. *Int Commun Heat Mass Transf* 37:34–38
9. van Rij J, Ameer T, Harman T (2009) The effect of viscous dissipation and rarefaction on rectangular microchannel convective heat transfer. *Int J Thermal Sci* 48:271–281
10. Hooman K, Hooman F, Famouri M (2009) Scaling effects for flow in micro-channels: variable property, viscous heating, velocity slip, and temperature jump. *Int Commun Heat Mass Transf* 36:192–196
11. Morini GL (2005) Viscous heating in liquid flows in microchannels. *Int J Heat Mass Transf* 48:3637–3647
12. Tunc G, Bayazitoglu Y (2001) Heat transfer in microtubes with viscous dissipation. *Int J Heat Mass Transf* 44:2395–2403
13. Magyari E, Barletta A (2007) Analytical series solution for the fully developed forced convection duct flow with frictional heating and variable viscosity. *Heat Mass Transf* 45:251–259
14. Jeong HE, Jeong JT (2006) Extended Graetz problem including streamwise conduction and viscous dissipation in microchannel. *Int J Heat Mass Transf* 49:2151–2157
15. El-Genk MS, Yang IH (2008) Friction numbers and viscous dissipation heating for laminar flows of water in microtubes. *J Heat Transf* 130:082405.1–082405.13
16. Yeoun YS, Yogesh J (2007) Conjugate heat transfer in an optical fiber coating process. *Numer Heat Transf Part A:Appl* 51:109–127
17. Hung YM (2009) A comparative study of viscous dissipation effect on entropy generation in single-phase liquid flow in microchannels. *Int J Therm Sci* 48:1026–1035
18. 3 M™ Novec™ 7600 Engineered Fluid, 3 M Electronics Markets Materials Division (2008)
19. Lelea D (2005) Some considerations on frictional losses evaluation of a water flow in microtubes. *Int Commun Heat Mass Transf* 32:964–973
20. Patankar SV (1980) *Numerical heat transfer fluid flow*. McGraw Hill, New York
21. Li Z, Huai X, Tao Y, Huanzhuo C (2007) Effects of thermal property variations on the liquid flow and heat transfer in microchannel heat sinks. *Appl Therm Eng* 27:2803–2814
22. Lee PS, Garimella SV (2006) Thermally developing flow and heat transfer in rectangular microchannels of different aspect ratios. *Int J Heat Mass Transf* 49:3060–3067